Extremophiles (2012) 16:57–66
DOI 10.1007/s00792-011-0405-0

ORIGINAL PAPER

Characterization of alcohol dehydrogenase (ADH12) from *Haloarcula marismortui*, an extreme halophile from the Dead Sea

Leanne M. Timpson · Diya Alsafadi · Cillín Mac Donnchadha · Susan Liddell · Michael A. Sharkey · Francesca Paradisi

Received: 20 July 2011 / Accepted: 6 October 2011 / Published online: 21 October 2011
© Springer 2011

Abstract Haloarchaeal alcohol dehydrogenases are of increasing interest as biocatalysts in the field of white biotechnology. In this study, the gene *adh12* from the extreme halophile *Haloarcula marismortui* (*Hm*ADH12), encoding a 384 residue protein, was cloned into two vectors: pRV1 and pTA963. The resulting constructs were used to transform host strains *Haloferax volcanii* (DS70) and (H1209), respectively. Overexpressed His-tagged recombinant *Hm*ADH12 was purified by immobilized metal-affinity chromatography (IMAC). The His-tagged protein was visualized by SDS-PAGE, with a subunit molecular mass of 41.6 kDa, and its identity was confirmed by mass spectrometry. Purified *Hm*ADH12 catalyzed the interconversion between alcohols and aldehydes and ketones, being optimally active in the presence of 2 M KCl. It was thermoactive, with maximum activity registered at 60°C. The NADP(H) dependent enzyme was haloalkaliphilic for the oxidative reaction with optimum activity at pH 10.0. It favored a slightly acidic pH of 6.0 for catalysis of the reductive reaction. *Hm*ADH12 was significantly more tolerant than mesophilic ADHs to selected organic solvents, making it a much more suitable biocatalyst for industrial application.

Keywords Alcohol dehydrogenase · Biocatalysis · Extremophile · Halophile · *Haloarcula marismortui* · *Haloferax volcanii* · Organic solvents

Communicated by L. Huang.

Electronic supplementary material The online version of this article (doi:10.1007/s00792-011-0405-0) contains supplementary material, which is available to authorized users.

L. M. Timpson · D. Alsafadi · C. Mac Donnchadha · F. Paradisi (✉)
Centre for Synthesis and Chemical Biology,
School of Chemistry and Chemical Biology,
University College Dublin, Belfield, Dublin 4, Ireland
e-mail: francesca.paradisi@ucd.ie

S. Liddell
Division of Animal Sciences,
University of Nottingham, Sutton Bonington Campus,
Loughborough LE12 5RD, UK

M. A. Sharkey
UCD School of Biomolecular and Biomedical Science,
Conway Institute, University College Dublin,
Belfield, Dublin 4, Ireland

Introduction

Alcohol dehydrogenases (ADHs) are a ubiquitous class of cofactor-dependent oxidoreductases (Reid and Fewson 1994). They have attracted much biotechnological interest for their ability to catalyze the interconversion between alcohols and aldehydes and ketones, one of the most widely used redox reactions in organic chemistry (Eichler 2001; Kroutil et al. 2004). As a result, novel ADHs find applications in the sustainable production of valuable building blocks and products in the pharmaceutical, agrochemical, food and fragrance industries. Most notably, ADHs are applied in the production of industrially valuable chiral alcohols, via asymmetric ketone reduction (Goldberg et al. 2007). ADHs can accomplish dynamic kinetic resolution (DKR) processes by which high yields (theoretically up to 100%) of a single enantiomer can be obtained. This has been demonstrated by Giacomini et al. (2007), who reported the efficient use of alcohol dehydrogenase from Horse Liver (HLADH) in the reduction of profenic aldehydes to industrially important optically pure alcohols. ADHs may also be applied in biosensor-based diagnostics and in fuel cell technology (Yakushi and Matsushita 2010).

Although enzymes are environmentally friendly catalysts with remarkable enantio- and regioselectivities, the industrial use of *mesophilic* enzymes, evolved to function in aqueous media and within narrow ranges of temperature and pH, is limited. Extremophiles, as a result of their ability to thrive in seemingly harsh environments, are exciting sources of robust biocatalysts with industrial applications (Adams et al. 1995). ADHs from both thermophiles and halophiles are important in industry where high temperatures and organic solvents are commonly used. The majority of extremophilic alcohol dehydrogenases reported have been thermophilic (Ammendola et al. 1992; Cannio et al. 1996; Machielsen et al. 2006, 2008; Pennacchio et al. 2008; Zhu et al. 2006), leaving relatively untapped the industrial potential of halophilic alcohol dehydrogenases, only one having been reported to date (Cao et al. 2008).

Extreme halophiles thrive in intensely saline environments, requiring between 2.5 and 5.2 M NaCl for optimal growth (Kamekura 1998). Evolved to contend with the osmotic pressure exerted by the hypersaline environment, the extreme halophiles of the family *Halobacteriaceae* accumulate molar concentrations of KCl intracellularly (Ginzburg et al. 1970). As a result of the "salt-in" strategy for osmotic adaptation, halophilic proteins are, in turn, adapted to remain soluble, stable and catalytically active in a hypersaline cytoplasm (Oren 2002). Distinct distinguishing features characteristic of halo-adapted proteins, with respect to their non-halo-adapted counterparts, include an excess of acidic residues over basic residues along with specific ion-binding sites located at subunit interfaces and an overall reduction in the protein hydrophobic content (Besir et al. 2005; Bracken et al. 2011; Richard et al. 2000). Recently, the structural and biochemical characterization of the lactate dehydrogenase-like malate dehydrogenase from the halophilic bacterium *Salinibacter ruber* has provided new insights into halophilic adaptation (Coquelle et al. 2010). The results presented protein haloadaptation as a gradual evolutionary response to high salt concentrations involving adaptive changes that allow for a balance between protein solubility, stability and activity to be established. Since both hypersaline and organic solvent environments exert a dehydrating effect on enzymes (Flam 1994), it has been hypothesized that mechanisms governing haloadaptation of proteins (Lanyi 1974; Mevarech et al. 2000; Zaccai et al. 1989) are transferrable to an organic solvent environment (Ruiz and De Castro 2007). This is supported by previous reports of halophilic enzymes exhibiting intrinsic organic solvent tolerance (Fukushima et al. 2005; Ruiz and De Castro 2007) making halophilic enzymes an exciting option for reactions that must be performed in aqueous/organic media.

While the heterologous overexpression of halophilic proteins in *E. coli* is often successful (Cendrin et al. 1993; Connaris et al. 1999; Domenech and Ferrer 2006; Johnsen and Schonheit 2004) it frequently results in the formation of inclusion bodies, thereby necessitating cumbersome solubilization and refolding procedures (Singh and Panda 2005). This may be avoided by employing a phylogenetically more closely related organism for the production of halophilic proteins. *Hfx. volcanii*, the genome sequence of which was recently published (Hartman et al. 2010), is an attractive host due to its ease of culture in salt media, its rapid doubling time in comparison to other haloarchaea (Robinson et al. 2005), its relative genetic stability (Lopez-Garcia et al. 1995) and its ease of transformation using PEG-mediated methods (Charlebois et al. 1987; Cline et al. 1989). Furthermore, the development of selectable markers (Allers et al. 2004; Bitan-Banin et al. 2003), an inducible promoter (Large et al. 2007) and a system for the conditional overexpression of halophilic proteins (Allers et al. 2010) has enhanced the appeal of *Hfx. volcanii* as an alternative expression host.

Here we report the production of a novel alcohol dehydrogenase ADH12 from *Har. marismortui*, the genome sequence of which was published by Baliga et al. (2004). We describe the cloning of *Har. marismortui adh12* into vectors pRV1, constructed by Large et al. (2007) and pTA963, constructed by Allers et al. (2010), the features of which have been previously documented. The subsequent overexpression of *Hm*ADH12 in *Hfx. volcanii* (DS70) (Wendoloski et al. 2001) and *Hfx. volcanii* (H1209) (Allers et al. 2010) is compared. The biochemical characterization and organic solvent tolerance of purified *Hm*ADH12 is also reported.

Materials and methods

Strains, vectors and culture conditions

All chemical reagents, unless stated otherwise, were purchased as analytical grade from Sigma-Aldrich. Restriction enzymes were purchased from New England Biolabs (USA). *E. coli* NovaBlue chemically competent cells and the pSTBlue-1 vector were purchased from Novagen (Germany). *E. coli* XL10-Gold® Ultracompetent cells were purchased from Stratagene (USA). *Har. marismortui* (ATCC 43049) genomic DNA was kindly donated by Dr. Bruno Franzetti, The Institute for Structural Biology (IBS), Grenoble (France). Dr. Peter A. Lund, School of Biosciences, University of Birmingham, Edgbaston (UK) kindly donated *Hfx. volcanii* (DS70) and the pRV1 vector. *Hfx. volcanii* (H1209) and the pTA963 vector were a kind donation from Dr. Thorsten Allers, Institute of Genetics,

School of Biology, University of Nottingham, Queen's Medical Centre, Nottingham (UK).

Transformed *E. coli* strains were cultured in Luria–Bertani (LB) agar and in LB broth containing ampicillin (100 μg/mL) at 37°C, 220 rpm. *Hfx. volcanii* strains were cultured at 45°C, 220 rpm. *Hfx. volcanii* (DS70) strains, harboring a pRV1 vector, were cultured in 18% MGM agar and in 18% salt water broth containing novobiocin (0.3 μg/mL) (Dyall-Smith 2008). *Hfx. volcanii* (H1209) strains, harboring a pTA963 vector, were cultured in *Hv*-YPC agar and in *Hv*-YPC broth (Allers et al. 2004).

Construction of expression plasmids (1) pRV1-*adh12*, (2) pTA963-*adh12*(A) and (3) pTA963-*adh12*(B)

1. The *adh12* gene was PCR amplified from *Har. marismortui* genomic DNA using Phusion™ DNA polymerase (Finnzymes, Finland). The oligonucleotide primers *Har. adh12* Fwd1 (5′-TTCATATGTTTCTGTATTTATATTCCATCTTTG-3′) and *Har. adh12* Rev1 (5′-TAGAATTCCGTATAGAACGATAACACTAGC-3′) were designed to incorporate *Nde*I and *Eco*RI restriction sites, respectively (underlined). The PCR product was cloned into the pSTBlue-1 vector using the AccepTor™ Vector kit (Novagen, Germany) according to the manufacturer's instructions. The resulting construct, designated as pSTBlue-1-*adh12*(A), was used to transform *E. coli* NovaBlue. The construct pSTBlue-1-*adh12*(A) was digested with *Nde*I and *Eco*RI and the gene *adh12* was cloned into the *Nde*I/*Eco*RI digested pRV1 vector. The resulting clone, designated as pRV1-*adh12* was propagated in *E. coli* XL10-Gold prior to transformation of *Hfx. volcanii* (DS70). As a control, *Hfx. volcanii* (DS70) was additionally transformed with the empty vector, pRV1.
2. The construct designated as pSTBlue-1-*adh12*(A) was digested with *Nde*I and *Eco*RI and the gene *adh12* was sub-cloned into the *Nde*I/*Eco*RI digested pTA963 vector. The resulting clone, designated as pTA963-*adh12*(A), was propagated in *E. coli* XL10-Gold prior to transformation of *Hfx. volcanii* (H1209).
3. The *adh12* gene was PCR amplified from the construct designated as pSTBlue-1-*adh12*(A) using the restriction site containing oligonucleotide primers *Har. adh12* Fwd2 (5′-TCCATGGGCATGTTTCTGTATTTATATTCC-3′) and *Har. adh12* Rev1 (5′-TAGAATTCCGTATAGAACGATAACACTAGC-3′), designed to incorporate the restriction sites *Nco*I and *Eco*RI, respectively (underlined). The PCR product was cloned into the pSTBlue-1 vector as described previously. The construct, designated as pSTBlue-1-*adh12*(B) was used to transform *E. coli* NovaBlue. Plasmid DNA isolated from selected clones was screened by *Nco*I/*Eco*RI restriction digest. pSTBlue-1-*adh12*(B) was digested with *Nco*I and *Eco*RI. The gene *adh12* was cloned into the pTA963 vector, digested with *Pci*I and *Eco*RI. The resulting construct, designated as pTA963-*adh12*(B), was propagated in *E. coli* XL10-Gold prior to transformation of *Hfx. volcanii* (H1209). As a control, *Hfx. volcanii* (H1209) was additionally transformed with the empty vector, pTA963.

Unless stated otherwise, plasmid DNA isolated from selected clones was screened by *Nde*I/*Eco*RI restriction enzyme digest. In each case, successful cloning was confirmed by DNA sequencing (Eurofins MWG Operon, Germany).

Transformation of competent cells

Chemically-competent *E. coli* cells were prepared and transformed according to standard procedures. Haloarchaeal competent cells were prepared according to the procedure outlined by Dyall-Smith (2008). *Hfx. volcanii* (DS70) and *Hfx. volcanii* (H1209) were transformed using the standard PEG-mediated transformation protocol according to the procedures outlined by Dyall-Smith (2008) and Allers et al. (2004), respectively. 18% MGM and *Hv*-YPC agar plates were sealed with parafilm and placed in a strong plastic bag. Colony formation was apparent after incubation at 45°C for 5–6 days.

Expression of *Hm*ADH12

Overnight starter cultures (5 mL) of *Hfx. volcanii* (DS70), transformed with pRV1-*adh12* and pRV1 were used to inoculate 270 mL 18% salt water broth, supplemented with novobiocin (0.3 μg/mL). Immediately after inoculation, protein expression was induced by addition of L-tryptophan to a final concentration of 5 mM. The cells were cultured for 4–5 days to OD_{600nm} values of approximately 3.5.

Similarly, overnight starter cultures of *Hfx. volcanii* (H1209) transformed with pTA963-*adh12*(A), pTA963-*adh12*(B) and pTA963 were used to inoculate 270 mL *Hv*-YPC broth. After 24 h, protein expression was induced as previously described. The culture was shaken for up to 7 h following induction.

Following protein production using both expression systems, cells were harvested by centrifugation, resuspended in 100 mM Tris–HCl buffer, pH 7.5, containing NaCl (2 M) and disodium EDTA (2 mM) (1 mL buffer was used to resuspend 100 mg cells). Cells were disrupted by sonication at 6 W, 4°C at intervals of 30 s until the lysate appeared transparent. After centrifugation (38,700×*g*, 4°C, 30 min) the supernatant was clarified by filtration and assayed for alcohol dehydrogenase activity.

Purification of *Hm*ADH12 by IMAC

The supernatant resulting from *Hfx. volcanii* (H1209) cells transformed with pTA963-*adh12*(B) was loaded at a flow rate of 1.0 mL/min onto a 1-mL His Trap™ FF Crude column pre-packed with Ni Sepharose™ 6 Fast Flow resin (GE Healthcare) and pre-charged with $NiSO_4$ (0.1 M). The column was equilibrated with 20 mM Tris–HCl buffer, pH 7.9, containing imidazole (20 mM) and NaCl (2 M). 20 mM Tris–HCl buffer, pH 7.9, containing NaCl (2 M) was passed through the column until all non-specifically bound protein was removed. An isocratic elution step using 20 mM Tris–HCl buffer, pH 7.9, containing NaCl (2 M) and disodium EDTA (0.5 mM) was applied to elute His-tagged protein. The purification was monitored by UV absorption at 280 nm. Fractions (2 mL) were collected and assayed spectrophotometrically for alcohol dehydrogenase activity. Active fractions were analyzed by SDS-PAGE using 12% polyacrylamide gels, stained with Coomassie brilliant blue R250 (Laemmli 1970). Staining and destaining was performed using the Stain/DeStain-XPress™ protein detection kit (Enzolve Technologies Ltd., Ireland). A broad range protein marker, P7702S, (2–212 kDa) (New England Biolabs, USA) was used for determination of relative molecular weight. Protein concentration was determined using Bradford protein assay dye reagent (Bio-Rad Laboratories GmbH, Germany) with bovine serum albumin as the standard (Bradford 1976). Fractions selected, based on purity and specific activity, were pooled and dialyzed overnight against 100 mM Tris–HCl buffer, pH 7.5, containing NaCl (2 M) at 4°C. Purified *Hm*ADH12 was routinely stored at −20°C.

Mass spectrometry

Proteins in 1D gel bands were reduced, carboxyamidomethylated and digested with Trypsin Gold (Promega) on a robotic platform for protein digestion (MassPREP station, Waters). The resulting peptides were analyzed by ESI–MS/MS after on-line separation on a PepMap C_{18} reversed-phase, 75 µm internal diameter, 15 cm column (LC Packings) on a CapLC system attached to a Q-TOF2 mass spectrometer equipped with a nanolockspray source (Waters) and operated with MassLynx Version 4.0 acquisition software. ProteinLynxGlobalServer version 2.0 (Waters) was used to process the uninterpreted MS data into peak list (pkl) files which were searched against all entries in the Swissprot and/or NCBInr databases using the web version of the MASCOT MS/MS ions search tool (Perkins et al. 1999). Carbamidomethylation of cysteine and oxidation of methionine were set as variable modifications. One missed cleavage by trypsin was accepted. Only protein identifications with probability-based MOWSE scores above a threshold of $P < 0.05$ were accepted.

Size exclusion chromatography

The molecular mass of the native *Hm*ADH12 was determined by size exclusion chromatography on a Superdex 200 high resolution 10/30 column with a total bed volume of 24 mL (GE Healthcare) equilibrated with 20 mM Tris–HCl buffer, pH 7.9, containing 2 M NaCl. Purified enzyme solution (100 µL) was injected and the experiment was run at a flow rate of 0.2 mL/min. Fractions were collected and those corresponding to the eluted peak were assayed for activity to confirm the protein was still correctly folded. Protein molecular weight markers (Sigma-Aldrich) used to prepare the calibration curve were β-amylase (200 kDa), yeast alcohol dehydrogenase (150 kDa), bovine serum albumin (66 kDa), carbonic anhydrase (29 kDa) and Cytochrome *c* (12.4 kDa), with Blue Dextran (2,000 kDa) being used to indicate the void volume. The samples for the calibration curve were run in 50 mM sodium phosphate buffer, pH 7.8, also containing 2 M NaCl (Yamamura et al. 2009).

Activity assays

Spectrophotometric activity measurements, based on the absorbance change of NAD(P)H at 340 nm, were routinely made in reaction mixtures (1 mL) at 50°C using a Varian Cary 50 Scan UV–visible spectrophotometer equipped with a Cary single cell peltier temperature controller. Unless otherwise stated, the reaction mixture for the oxidative step contained ethanol (100 mM), $NADP^+$ (1 mM), enzyme sample (10 µL) and 50 mM glycine–NaOH buffer, pH 10.0, containing KCl (2 M). The reaction mixture for the reductive step routinely contained acetaldehyde (50 mM), NADPH (0.1 mM), enzyme sample (10 µL) and 50 mM citric acid–K_2HPO_4 buffer, pH 6.0, containing KCl (2 M). Buffers were equilibrated at 50°C prior to testing. One unit of ADH corresponded to the amount of enzyme required to oxidize or reduce 1 µmol of NADPH or $NADP^+$ per min, respectively.

Characterization of *Hm*ADH12

Oxidative reaction optima were determined on assaying *Hm*ADH12 for activity against 1-propanol (100 mM) with $NADP^+$ (1 mM) using the buffers: 50 mM sodium pyrophosphate, pH 8.0, containing 2–4 M KCl, 50 mM Tris–HCl, pH 8.0, containing 2–4 M NaCl and 50 mM glycine–NaOH, pH 9.0 and 10.0, containing 2–4 M KCl and NaCl. Reductive reaction optima were determined on assaying *Hm*ADH12 for activity against acetaldehyde

(50 mM) with NADPH (0.1 mM) using the buffers: 50 mM citric acid–K_2HPO_4, pH 5.0 and 6.0, containing 2–4 M KCl; 50 mM potassium phosphate, pH 7.0, containing 2–4 M KCl; and 50 mM Tris–HCl, pH 8.0, containing 2–4 M KCl. The optimum temperature for activity was determined by performing the standard assay for the oxidative reaction between 20 and 80°C. The cofactor dependency of the enzyme was investigated by screening *Hm*ADH12 for activity against ethanol (100 mM) and 1-propanol (100 mM) using both nicotinamide cofactors (1 mM) in the oxidative reaction, using the previously mentioned buffers. *Hm*ADH12 was screened for activity against alcohol substrates methanol, ethanol, 1-propanol, 1-butanol, 1-pentanol, 2-propanol, 2-butanol, glycerol and glucose (100 mM). The effect of storage temperature on *Hm*ADH12 activity was monitored by assaying purified enzyme stored at 4°C and at −20°C for activity. To investigate organic solvent tolerance *Hm*ADH12, HLADH and YADH were incubated for 24 h at 4°C with 10% polar aprotic organic solvents dimethyl sulfoxide (DMSO), acetonitrile (ACN) and tetrahydrofuran (THF). The enzymes were assayed for activity at time zero and after incubation. HLADH and YADH were assayed in 100 mM sodium pyrophosphate buffer, pH 8.8 using NAD^+ (1 mM). Kinetic measurements for the oxidative reaction enzyme assays were performed over a range of ethanol concentrations (0–250 mM) and $NAD(P)^+$ concentrations (0–3.5 mM). For the reductive reaction enzyme assays were performed over a range of acetaldehyde concentrations (0–200 mM) and NAD(P)H concentrations (0–0.3 mM). Hanes–Woolf linear plots of the Michaelis–Menten equation were used to determine kinetic parameters of the enzyme. Kinetic data were plotted using SigmaPlot (Version 11.0).

Results and discussion

Expression of *Hm*ADH12

Several haloarchaeal proteins have been successfully solubilized and reactivated from inclusion bodies following heterologous overexpression in *E. coli*. However, this approach is not successful for all halophilic proteins, particularly in cases where the conditions for reactivation of a given protein from *E. coli* inclusion bodies are unknown. Such was the case for *Hm*ADH12, which was initially heterologously overexpressed as *E. coli* inclusion bodies. The protein was solubilized and attempts were made to reactivate the protein via direct dilution and dialysis against a range of buffers varying in pH and salt concentration, supplemented with recommended refolding additives. However, ADH activity was never detected. The inactivity appeared to be due to incorrect protein folding or unsuitable assay conditions since bioinformatic analysis confirmed that the necessary conserved residues for the binding of structural and catalytic zinc, along with the binding of the nicotinamide cofactor, were present in the protein sequence.

Table 1 Effect of expression system on *Hm*ADH12 activity (crude extract) and culture growth time

Strain/vector	Protein conc. (mg/mL)	S.A. (U/mg)	Time (days)
DS70/pRV1	11.93	0.021	5–6
H1209/pTA963(A)	7.57	0.020	2.5
H1209/pTA963(B)	7.84	0.015	2.5

Alternatively, two *Hfx. volcanii* expression systems were investigated for the soluble expression of *Hm*ADH12: *Hfx. volcanii* (DS70), coupled with the vector pRV1 and *Hfx. volcanii* (H1209), coupled with the vector pTA963. The gene *adh12* was cloned into pTA963 such that in one case (A) the hexahistidine tag was removed to facilitate direct comparison between expression systems without potential interference from a His-tag, and in the second case (B) it was retained to facilitate purification of *Hm*ADH12 from endogenous *Hfx. volcanii* proteins. Both expression systems yielded soluble *Hm*ADH12 that actively catalyzed the interconversion between alcohols and aldehydes and ketones. In each case the control supernatant was inactive. The DS70/pRV1 and H1209/pTA963 systems were compared in terms of enzyme specific activity of the crude extract, protein concentration and culture growth time (Table 1). While the overall efficiency of the systems was comparable, a highly desirable advantage of using the (H1209)/pTA963 system was the reduction in overall culture time required. This was attributed to the selection of transformed *Hfx. volcanii* (H1209) cells by *pyr*E2 and *hdr*B markers, featured in the pTA963 vector, that maintain plasmids in rich medium without the requirement for antibiotics. This was in contrast to the DS70/pRV1 system, in which selection was based on resistance to novobiocin, an antibiotic known to impair cell growth (Allers et al. 2010).

Purification and identity of *Hm*ADH12

Since it is unaffected by high salt concentrations, IMAC (Porath et al. 1975) is a valuable tool for the purification of halophilic proteins, which are often inactivated at salt concentrations below 1 M (Margesin and Schinner 2001). *Hm*ADH12 was purified in a single-step using IMAC with Ni^{2+} as the immobilized ion. Several active fractions were collected with a maximum specific activity of 0.41 U/mg and a purification figure of 16-fold. The expected 41.6 kDa

His-tagged protein was visualized by 12% SDS-PAGE (Fig. 1). As is the case for many halophilic proteins, the apparent molecular weight of *Hm*ADH12 was overestimated when visualized by SDS-PAGE. This can be attributed to the excess of negative charge, which affects the migration of halophilic proteins through the gel matrix (Madern et al. 2000); *Hm*ADH12 featured 16% acidic residues, a figure consistent with those reported for other halophilic proteins (Camacho et al. 2002; Cao et al. 2008). The visualized band was subsequently excised from the gel and analyzed by mass spectrometry, which identified peptides belonging to the predicted *Hm*ADH12 with a subunit molecular mass of 41.6 kDa. Following purification, the purest, most active fractions were pooled and dialyzed overnight to remove EDTA, known to have an inhibitory effect on zinc-dependent ADHs (Vallee and Hoch 1957). The specific activity after dialysis of 0.45 U/mg was approximately 10% greater than that observed immediately after purification in the most active fraction, indicating a final 17-fold purification of *Hm*ADH12. The molecular mass of the native *Hm*ADH12 was estimated to be 180 kDa from the calibration curve, which indicated a tetrameric quaternary structure (theoretical value 167 kDa). Purified *Hm*ADH12 was routinely stored in a buffer containing 2 M NaCl. This concentration was selected based on a literature review of halophilic proteins from *Har. marismortui*, which strongly related the salt concentration required for maximum activity to that of a correctly folded enzyme (Brasen and Schonheit 2005; Muller-Santos et al. 2009; Rao et al. 2009).

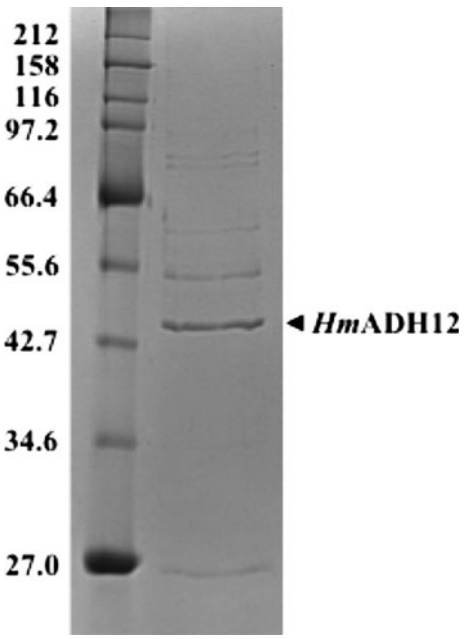

Fig. 1 SDS-PAGE visualization of *Hm*ADH12. *Lane 1* broad range protein marker P7702S, *Lane 2* *Hm*ADH12. The protein concentration of the purified sample was 0.58 mg/mL. Molecular masses in kDa are indicated on the *left*. An *arrowhead* indicates the position of *Hm*ADH12

Characterization of *Hm*ADH12

Purified *Hm*ADH12 was most stable when stored at −20°C, retaining approximately 80% of its original activity after 10 days. In contrast, enzyme stored at 4°C lost half of its original activity over the same period (Fig. 2).

In terms of cofactor dependency, *Hm*ADH12 exhibited a definite preference for $NADP^+$ for activity. At pH 10.0, however, minor activity (75% less than that detected with $NADP^+$) was detected with NAD^+. A preference for NADP(H) over NAD(H) is often seen as a drawback from a biotechnological viewpoint due to the lability and expense of the phosphorylated cofactors. The dependency can be shifted to principally accommodate NAD(H) by random or site-directed mutagenesis (Rodriguez-Arnedo et al. 2005). Alternatively, the perceived expense of phosphorylated cofactors can be drastically reduced given an efficient cofactor regeneration system is in place (Weckbecker et al. 2010).

Screening of alcohol substrates revealed that *Hm*ADH12 preferentially accepted short-chain alcohols. 100% activity against ethanol corresponded to a specific activity of 0.18 U/mg. With respect to ethanol, *Hm*ADH12 displayed 137% activity against 1-propanol, 117% activity against 1-butanol, 74% activity against 1-pentanol and 43% activity against the branched alcohol, 2-butanol. The enzyme did not accept methanol, 2-propanol, glycerol or glucose as substrates.

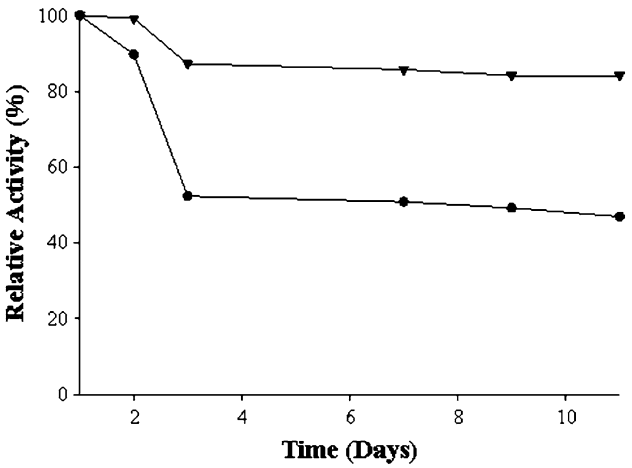

Fig. 2 The effect of storage temperature on the stability of *Hm*ADH12. *Hm*ADH12 was stored at −20°C (*down triangle*) and 4°C (*circle*) and its activity monitored. The results were expressed as relative activities (%). 100% activity corresponded to a specific activity of 0.27 U/mg

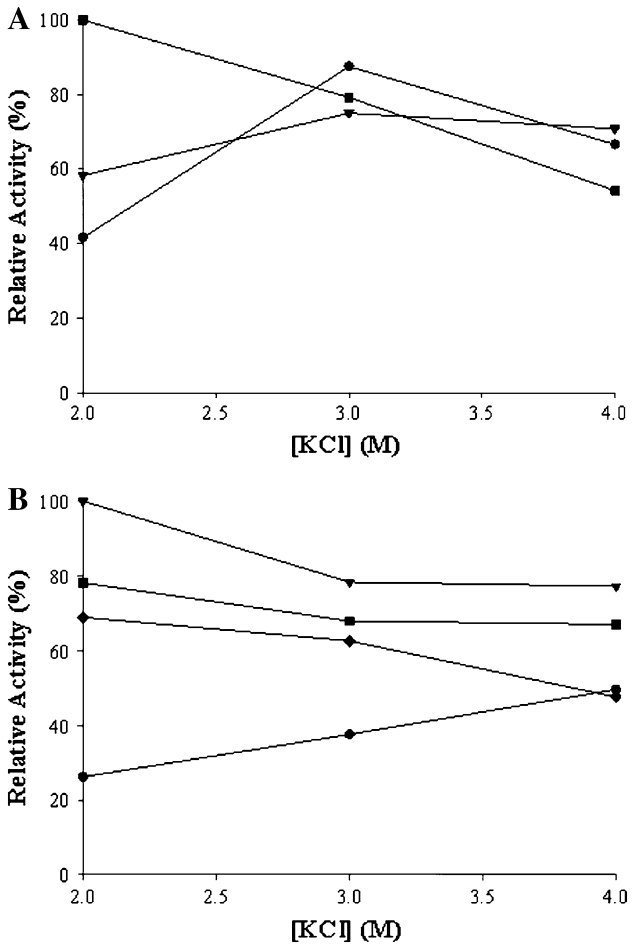

Fig. 3 **a** Optimum pH and KCl concentration for catalysis of the oxidative reaction by *Hm*ADH12. Buffers used were 50 mM sodium pyrophosphate, pH 8.0 (*circle*), containing 2–4 M KCl and 50 mM glycine–NaOH, pH 9.0 (*down triangle*) and 10.0 (*square*), containing 2–4 M KCl. The results were expressed as relative activities (%). 100% activity corresponded to a specific activity of 0.02 U/mg. **b** Optimum pH and KCl concentration for catalysis of the reductive reaction by *Hm*ADH12. Buffers used were 50 mM citric acid–K_2HPO_4, pH 5.0 (*circle*) and 6.0 (*down triangle*), containing 2–4 M KCl, 50 mM potassium phosphate, pH 7.0 (*square*), containing 2–4 M KCl and 50 mM Tris–HCl, pH 8.0 (*diamond*), containing 2–4 M KCl. The results were expressed as relative activities (%). 100% activity corresponded to a specific activity of 0.09 U/mg

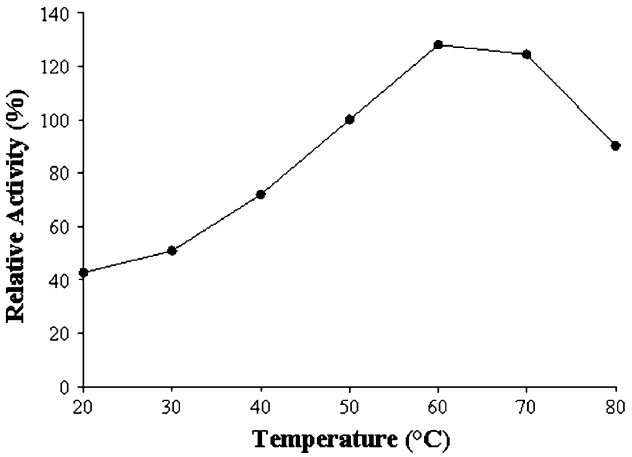

Fig. 4 Effect of temperature on *Hm*ADH12 activity. Enzyme activity was examined under standard assay conditions at temperatures 20°C through to 80°C. The results were expressed as relative activities (%). 100% activity corresponded to a specific activity of 0.08 U/mg

The optimum conditions for the activity of *Hm*ADH12 in terms of pH, salt type and salt concentration were investigated. Considering the catalytic mechanism for the oxidative and reductive reactions, it was anticipated that the enzyme would catalyze the oxidative reaction optimally in an alkaline environment and vice versa. In the oxidative reaction, maximum activity was observed at pH 10.0 (Fig. 3a). Conversely, the enzyme favored a slightly acidic pH for catalysis of the reductive reaction, with maximum activity observed at pH 6.0 (Fig. 3b). *Hm*ADH12 was approximately twice as active with KCl than with NaCl. While not observed with all halophilic enzymes, it is common for some to be more active with KCl than with NaCl (Bischoff and Rodwell 1996). At pH 10.0, *Hm*ADH12 was optimally active with 2 M KCl and above this concentration a steady decrease in activity was recorded. Upon decreasing the concentration to 1 M KCl, approximately 50% of the optimum activity was detected and when no salt was added to the reaction mixture the enzyme was inactive (data not shown). In addition to being halophilic, *Hm*ADH12 was also thermoactive with a maximum activity registered at 60°C (Fig. 4). Thermoactivity is a common characteristic of halophilic proteins owing to shared structural features associated with both haloadaptation and life at high temperatures (Dym et al. 1995). The capability of withstanding combined physical and geochemical extremes adds another dimension to the potential application of *Hm*ADH12 in industry, where multiple stressors may be present (Rothschild and Mancinelli 2001). *Hm*ADH12 represents the first alcohol dehydrogenase to be expressed, purified and characterized from *Har. marismortui*. The first reported haloarchaeal ADH was from *Natronomonas pharaonis*. Like *Hm*ADH12, *Np*ADH was haloalkaliphilic and thermoactive exhibiting maximum activity at pH 9.0 with 4 M KCl at 70°C (Cao et al. 2008).

Enzyme kinetic experiments revealed that *Hm*ADH12 followed Michaelis–Menten kinetics with $NADP^+$, NADPH and with acetaldehyde as a substrate in the reductive reaction (Table 2). The enzyme was positively co-operative with ethanol as a substrate in the oxidative reaction, with a Hill coefficient of 1.3 ± 0.1. The enzyme appeared to preferentially catalyze the reductive reaction and therefore may be of use in the production of chiral alcohols.

Table 2 Kinetic parameters of *Hm*ADH12

Substrate/cofactor	K_m (mM)	V_{max} (U/mg)
Acetaldehyde	5.1 ± 0.9	1.63 ± 0.02
$NADP^+$	0.101 ± 0.006	0.393 ± 0.004
NADPH	0.029 ± 0.002	2.72 ± 0.03

Following incubation with 10% THF, *Hm*ADH12 and the mesophilic ADHs from horse liver (HLADH) and from yeast (YADH) were deactivated. However, *Hm*ADH12 was highly stable in the presence of 10% DMSO and ACN, retaining 78 and 69% activity, respectively, following incubation. The tolerance of *Hm*ADH12 is comparable to that of a protease from the haloalkaliphilic *Natrialba magadii*, which was stable in the presence of 15% organic solvents DMSO and DMF (Ruiz and De Castro 2007). In contrast, the mesophilic ADHs tested did not exhibit the same degree of stability. HLADH retained 73% activity following incubation with ACN, but displayed only minor activity following incubation with DMSO. The opposite was observed with YADH, which retained 72% activity after incubation with DMSO and only 38% activity following incubation with ACN. These data support the hypothesis that shortcomings associated with the use of mesophilic enzymes in organic solvent may be overcome by employing a halophilic counterpart.

Conclusion

We present the efficient and consistent production of *Hm*ADH12, which catalyzes the industrially important interconversion between alcohols and aldehydes and ketones. In this way, a green alternative to conventional metal-based catalysis is presented. The intrinsic tolerance of the enzyme to 10% organic solvents, coupled with its thermoactivity guarantees reactant and product solubility. Though the enzyme shows potential as a biocatalyst, the overall stability of the enzyme would need to be improved by means of directed evolution to make it a more robust biocatalyst.

Acknowledgments Science Foundation Ireland (SFI), the Irish Research Council for Science, Engineering and Technology (IRCSET), Merck and the Islamic Development Bank (IsDB) supported this work. We thank Dr. Thorsten Allers for specialist advice on the *Hfx. volcanii* (H1209)/pTA963 expression system.

References

Adams MWW, Perler FB, Kelly RM (1995) Extremozymes: expanding the limits of biocatalysis. Nat Biotechnol 13:662–668

Allers T, Ngo H-P, Mevarech M, Lloyd RG (2004) Development of additional selectable markers for the halophilic archaeon *Haloferax volcanii* based on the *leuB* and *trpA* genes. Appl Environ Microbiol 70:943–953

Allers T, Barak S, Liddell S, Wardell K, Mevarech M (2010) Improved strains and plasmid vectors for conditional overexpression of his-tagged proteins in *Haloferax volcanii*. Appl Environ Microbiol 76:1759–1769

Ammendola S, Raia CA, Caruso C, Camardella L, D' Auria S, De Rosa M, Rossi M (1992) Thermostable NAD^+-dependent alcohol dehydrogenase from *Sulfolobus solfataricus*: gene and protein sequence determination and relationship to other alcohol dehydrogenases. Biochemistry 31:12514–12523

Baliga NS, Bonneau R, Facciotti MT, Pan M, Glusman G, Deutsch EW, Shannon P, Chiu Y, Weng RS, Gan RR, Hung P, Date SV, Marcotte E, Hood L, Ng WV (2004) Genome sequence of *Haloarcula marismortui*: a halophilic archaeon from the Dead Sea. Genome Res 14:2221–2234

Besir H, Zeth K, Bracher A, Heider U, Ishibashi M, Tokunaga M, Oesterhelt D (2005) Structure of a halophilic nucleoside diphosphate kinase from *Halobacterium salinarum*. FEBS Lett 579:6595–6600

Bischoff KM, Rodwell VW (1996) 3-Hydroxy-3-methylglutaryl-coenzyme A reductase from *Haloferax volcanii*: purification, characterization, and expression in *Escherichia coli*. J Bacteriol 178:19–23

Bitan-Banin G, Ortenberg R, Mevarech M (2003) Development of a gene knockout system for the halophilic archaeon *Haloferax volcanii* by use of the *pyrE* gene. J Bacteriol 185:772–778

Bracken CD, Neighbor AM, Lamlenn KK, Thomas GC, Schubert HL, Whitby FG, Howard BR (2011) Crystal structures of a halophilic archaeal malate synthase from *Haloferax volcanii* and comparisons with isoforms A and G. BMC Struct Biol 11:1–19

Bradford MM (1976) A rapid and sensitive method for the quantitation of microgram quantities of protein utilizing the principle of protein-dye binding. Anal Biochem 72:248–254

Brasen C, Schonheit P (2005) AMP-forming acetyl-CoA synthetase from the extremely halophilic archaeon *Haloarcula marismortui*: purification, identification and expression of the encoding gene, and phylogenetic affiliation. Extremophiles 9:355–365

Camacho M, Rodriguez-Arnedo A, Bonete M-J (2002) NADP-dependent isocitrate dehydrogenase from the halophilic archaeon *Haloferax volcanii*: cloning, sequence determination and overexpression in *Escherichia coli*. FEMS Microbiol Lett 209:155–160

Cannio R, Fiorentino G, Carpinelli P, Rossi M, Bartolucci S (1996) Cloning and overexpression in *Escherichia coli* of the genes encoding NAD-dependent alcohol dehydrogenase from two *Sulfolobus* species. J Bacteriol 178:301–305

Cao Y, Liao L, Xu X, Oren A, Wang C, Zhu X, Wu M (2008) Characterization of alcohol dehydrogenase from the haloalkaliphilic archaeon *Natronomonas pharaonis*. Extremophiles 12:471–476

Cendrin F, Chroboczek J, Zaccai G, Eisenberg H, Mevarech M (1993) Cloning, sequencing, and expression in *Escherichia coli* of the gene coding for malate dehydrogenase of the extremely halophilic archaebacterium *Haloarcula marismortui*. Biochemistry 32:4308–4313

Charlebois RL, Lam WL, Cline SW, Doolittle WF (1987) Characterization of pHV2 from *Halobacterium volcanii* and its use in demonstrating transformation of an archaebacterium. Proc Natl Acad Sci USA 84:8530–8534

Cline SW, Lam WL, Charlebois RL, Schalkwyk LC, Doolittle WF (1989) Transformation methods for halophilic archaebacteria. Can J Microbiol 35:148–152

Connaris H, Chaudhuri JB, Danson MJ, Hough DW (1999) Expression, reactivation, and purification of enzymes from *Haloferax volcanii* in *Escherichia coli*. Biotechnol Bioeng 64:38–45

Coquelle N, Talon R, Juers DH, Girard E, Kahn R, Madern D (2010) Gradual adaptive changes of a protein facing high salt concentrations. J Mol Biol 404:493–505

Domenech J, Ferrer J (2006) A new d-2-hydroxyacid dehydrogenase with dual coenzyme-specificity from *Haloferax mediterranei*, sequence analysis and heterologous overexpression. Biochim Biophys Acta Gen Subj 1760:1667–1674

Dyall-Smith M (2008) Protocols for haloarchaeal genetics The Halohandbook Version 7

Dym O, Mevarech M, Sussman JL (1995) Structural features that stabilize halophilic malate dehydrogenase from an archaebacterium. Science 267:1344–1346

Eichler J (2001) Biotechnological uses of archaeal extremozymes. Biotechnol Adv 19:261–278

Flam F (1994) The chemistry of life at the margins. Science 265:471–472

Fukushima T, Mizuki T, Echigo A, Inoue A, Usami R (2005) Organic solvent tolerance of halophilic α-amylase from a haloarchaeon, *Haloarcula* sp. strain S-1. Extremophiles 9:85–89

Giacomini D, Galletti P, Quintavalla A, Gucciardo G, Paradisi F (2007) Highly efficient asymmetric reduction of arylpropionic aldehydes by Horse Liver alcohol dehydrogenase through dynamic kinetic resolution. Chem Commun 21:4038–4040

Ginzburg M, Sachs L, Ginzburg BZ (1970) Ion metabolism in a Halobacterium. I. Influence of age of culture on intracellular concentrations. J Gen Physiol 55:187–207

Goldberg K, Schroer K, Lütz S, Liese A (2007) Biocatalytic ketone reduction—a powerful tool for the production of chiral alcohols—part I: processes with isolated enzymes. Appl Microbiol Biotechnol 76:237–248

Hartman AL, Norais C, Badger JH, Delmas S, Haldenby S, Madupu R, Robinson J, Khouri H, Ren Q, Lowe TM, Maupin-Furlow J, Pohlschroder M, Daniels C, Pfeiffer F, Allers T, Eisen JA (2010) The complete genome sequence of *Haloferax volcanii* DS2, a model archaeon. PLoS One 5:e9605

Johnsen U, Schonheit P (2004) Novel xylose dehydrogenase in the halophilic archaeon *Haloarcula marismortui*. J Bacteriol 186: 6198–6207

Kamekura M (1998) Diversity of extremely halophilic bacteria. Extremophiles 2:289–295

Kroutil W, Mang H, Edegger K, Faber K (2004) Recent advances in the biocatalytic reduction of ketones and oxidation of sec-alcohols. Curr Opin Chem Biol 8:120–126

Laemmli UK (1970) Cleavage of structural proteins during the assembly of the head of bacteriophage T4. Nature 227:680–685

Lanyi J (1974) Salt-dependent properties of proteins from extremely halophilic bacteria. Microbiol Mol Biol Rev 38:272–290

Large A, Stamme C, Lange C, Duan Z, Allers T, Soppa J, Lund PA (2007) Characterization of a tightly controlled promoter of the halophilic archaeon *Haloferax volcanii* and its use in the analysis of the essential cct1 gene. Mol Microbiol 66:1092–1106

Lopez-Garcia P, St Jean A, Amils R, Charlebois RL (1995) Genomic stability in the archaeae *Haloferax volcanii* and *Haloferax mediterranei*. J Bacteriol 177:1405–1408

Machielsen R, Uria AR, Kengen SWM, van der Oost J (2006) Production and characterization of a thermostable alcohol dehydrogenase that belongs to the aldo-keto reductase superfamily. Appl Environ Microbiol 72:233–238

Machielsen R, Leferink NGH, Hendriks A, Brouns SJJ, Hennemann H-G, Daussmann T, van der Oost J (2008) Laboratory evolution of *Pyrococcus furiosus* alcohol dehydrogenase to improve the production of (2S, 5S)-hexanediol at moderate temperatures. Extremophiles 12:587–594

Madern D, Ebel C, Zaccai G (2000) Halophilic adaptation of enzymes. Extremophiles 4:91–98

Margesin R, Schinner F (2001) Potential of halotolerant and halophilic microorganisms for biotechnology. Extremophiles 5:73–83

Mevarech M, Frolow F, Gloss LM (2000) Halophilic enzymes: proteins with a grain of salt. Biophys Chem 86:155–164

Muller-Santos M, de Souza EM, Pedrosa F, Mitchell DA, Longhi S, Carriere F, Canaan S, Krieger N (2009) First evidence for the salt-dependent folding and activity of an esterase from the halophilic archaea *Haloarcula marismortui*. Biochim Biophys Acta 1791:719–729

Oren A (2002) Diversity of halophilic microorganisms: Environments, phylogeny, physiology, and applications. J Ind Microbiol Biotechnol 28:56–63

Pennacchio A, Pucci B, Secundo F, La Cara F, Rossi M, Raia CA (2008) Purification and characterization of a novel recombinant highly enantioselective short-chain NAD(H)-dependent alcohol dehydrogenase from *Thermus thermophilus*. Appl Environ Microbiol 74:3949–3958

Perkins DN, Pappin DJC, Creasy DM, Cottrell JS (1999) Probability-based protein identification by searching sequence databases using mass spectrometry data. Electrophoresis 20:3551–3567

Porath J, Carlsson J, Olsson I, Belfrage G (1975) Metal chelate affinity chromatography, a new approach to protein fractionation. Nature 258:598–599

Rao L, Zhao X, Pan F, Li Y, Xue Y, Ma Y, Lu JR (2009) Solution behaviour and activity of a halophilic esterase under high salt concentration. PLoS One 4:e6980

Reid MF, Fewson CA (1994) Molecular characterization of microbial alcohol dehydrogenases. Crit Rev Microbiol 20:13–56

Richard SB, Madern D, Garcin E, Zaccai G (2000) Halophilic adaptation: novel solvent protein interactions observed in the 2.9 and 2.6 Å resolution structures of the wild type and a mutant of malate dehydrogenase from *Haloarcula marismortui*. Biochemistry 39:992–1000

Robinson JL, Pyzyna B, Atrasz RG, Henderson CA, Morrill KL, Burd AM, DeSoucy E, Fogleman RE III, Naylor JB, Steele SM, Elliott DR, Leyva KJ, Shand RF (2005) Growth kinetics of extremely halophilic Archaea (family *Halobacteriaceae*) as revealed by arrhenius plots. J Bacteriol 187:923–929

Rodriguez-Arnedo A, Camacho M, Llorca F, Bonete M-J (2005) Complete reversal of coenzyme specificity of isocitrate dehydrogenase from *Haloferax volcanii*. Protein J 24:259–266

Rothschild LJ, Mancinelli RL (2001) Life in extreme environments. Nature 409:1092–1101

Ruiz DM, De Castro RE (2007) Effect of organic solvents on the activity and stability of an extracellular protease secreted by the haloalkaliphilic archaeon *Natrialba magadii*. J Ind Microbiol Biotechnol 34:111–115

Singh SM, Panda AK (2005) Solubilization and refolding of bacterial inclusion body proteins. J Biosci Bioeng 99:303–310

Vallee BL, Hoch FL (1957) Zinc in horse liver alcohol dehydrogenase. J Biol Chem 225:185–195

Weckbecker A, Groger H, Hummel W (2010) Regeneration of nicotinamide coenzymes: principles and applications for the synthesis of chiral compounds. Adv Biochem Eng/Biotechnol 120:195–242

Wendoloski D, Ferrer C, Dyall-Smith ML (2001) A new simvastatin (mevinolin)-resistance marker from *Haloarcula hispanica* and a new *Haloferax volcanii* strain cured of plasmid pHV2. Microbiology 147:959–964

Yakushi T, Matsushita K (2010) Alcohol dehydrogenase of acetic acid bacteria: structure, mode of action, and applications in biotechnology. Appl Microbiol Biotechnol 86:1257–1265

Yamamura A, Ichimura T, Kamekura M, Mizuki T, Usami R, Makino T, Ohtsuka J, Miyazono K, Okai M, Nagata K, Tanokura M

(2009) Molecular mechanism of distinct salt-dependent enzyme activity of two halophilic nucleoside diphosphate kinases. Biophys J 96:4692–4700

Zaccai G, Cendrin F, Haik Y, Borochov N, Eisenberg H (1989) Stabilization of halophilic malate dehydrogenase. J Mol Biol 208:491–500

Zhu D, Malik HT, Hua L (2006) Asymmetric ketone reduction by a hyperthermophilic alcohol dehydrogenase. The substrate specificity, enantioselectivity and tolerance of organic solvents. Tetrahedron Asymmetry 17:3010–3014